A genomic rearrangement resulting in a tandem duplication is associated with split hand–split foot malformation 3 (SHFM3) at 10q24

Xavier J. de Mollerat[1,2], Fiorella Gurrieri[3], Chad T. Morgan[1], Eugenio Sangiorgi[3],
David B. Everman[1,2], Paola Gaspari[3], Jeanne Amiel[4], Michael J. Bamshad[5], Robert Lyle[6],
Jean-Louis Blouin[6], Judith E. Allanson[7], Bernard Le Marec[8], Melba Wilson[9],
Nancy E. Braverman[10], Uppala Radhakrishna[6], Celia Delozier-Blanchet[6], Albert Abbott[2],
Vincent Elghouzzi[4], Stylianos Antonarakis[6], Roger E. Stevenson[1,2], Arnold Munnich[4],
Giovanni Neri[3] and Charles E. Schwartz[1,2,*]

[1]Center for Molecular Studies, J.C. Self Research Institute of Human Genetics, Greenwood Genetic Center,
Greenwood, SC, USA, [2]Department of Genetics and Biochemistry, Clemson University, Clemson, SC, USA,
[3]Istituto di Genetica Medica, Università Cattolica, Roma, Italy, [4]Département de Génétique and Unité INSERM U-393
Hôpital Necker-Enfants Malades, Paris, France, [5]Department of Genetics, School of Medicine, University of Utah,
Salt Lake City, UT, USA, [6]Division of Medical Genetics, University of Geneva Medical School, Geneva, Switzerland,
[7]Department of Genetics, Children's Hospital of Eastern Ontario Research Institute, Ottawa, Ontario, Canada,
[8]Faculté de Médecine de Rennes I, Service de Pediatrie-Génétique Medicale, Rennes, France, [9]Center for Human
Genetics, Bar Harbor, ME, USA and [10]John Hopkins University, School of Medicine, Baltimore, MD, USA

Split hand–split foot malformation (SHFM) is characterized by hypoplasia/aplasia of the central digits with fusion of the remaining digits. SHFM is usually an autosomal dominant condition and at least five loci have been identified in humans. Mutation analysis of the *DACTYLIN* gene, suspected to be responsible for SHFM3 in chromosome 10q24, was conducted in seven SHFM patients. We screened the coding region of *DACTYLIN* by single-strand conformation polymorphism and sequencing, and found no point mutations. However, Southern, pulsed field gel electrophoresis and dosage analyses demonstrated a complex rearrangement associated with a ~0.5 Mb tandem duplication in all the patients. The distal and proximal breakpoints were within an 80 and 130 kb region, respectively. This duplicated region contained a disrupted extra copy of the *DACTYLIN* gene and the entire *LBX1* and β-*TRCP* genes, known to be involved in limb development. The possible role of these genes in the SHFM3 phenotype is discussed.

INTRODUCTION

Ectrodactyly or split hand–split foot malformation (SHFM) is a human limb malformation characterized by hypoplasia/aplasia of the central digital rays and variable fusion of the remaining digits (MIM 183600). The condition occurs in 1 in 8500–25 000 newborns and accounts for 8–17% of all limb reduction defects (1–5). SHFM is clinically heterogeneous, presenting in both non-syndromic and syndromic forms. The non-syndromic form can be isolated (type I) or associated with long bone

deficiency (type II—also called SHFLD; MIM 119100) (6). Among the several syndromes in which SHFM occurs, the most common is the EEC (ectrodactyly, ectodermal dysplasia, cleft lip/palate) syndrome (MIM 129900) (7).

When familial, SHFM is usually inherited in an autosomal dominant manner with incomplete penetrance, variable expressivity and segregation distortion with excessive transmission from affected males to sons (6,8–10). An X-linked form has been reported in a single family, and autosomal recessive inheritance has also been described (11–14). To date, five loci

*To whom correspondence should be addressed at: Center for Molecular Studies, J.C. Self Research Institute of Human Genetics, One Gregor Mendel Circle, Greenwood, SC 29646, USA. Tel: +1 8649418140; Fax: +1 8643881707; Email: schwartz@ggc.org

for non-syndromic and syndromic SHFM have been identified based upon linkage mapping and/or cytogenetic abnormalities: SHFM1 on chromosome 7q21.3–q22.1 (15,16), SHFM2 on Xq26 (11,13), SHFM3 on 10q24 (17,18), SHFM4 on 3q27 (19) and SHFM5 on 2q31 (20,21). *P63*, the gene responsible for SHFM4 on 3q27, is the only gene thus far identified in human SHFM (19,22). Interestingly, *P63* mutations and abnormalities at the SHFM1 locus cause both syndromic and non-syndromic SHFM (22,23). In contrast, only non-syndromic SHFM has been mapped to the SHFM3 locus (17,18,24).

Studies of the naturally occurring *Dactylaplasia* (Dac) mouse, which has an SHFM-like phenotype, have been critical to investigation of the SHFM3 locus. The mouse phenotype bears striking similarity to typical human SHFM, with absence of central digits, underdevelopment or absence of metacarpal/metatarsal bones and syndactyly (25). The Dac phenotype is inherited as an autosomal semidominant trait, with the more severe phenotype (e.g. monodactyly) occurring in homozygotes (26,27). The Dac locus was mapped to chromosome 19 in a region syntenic to chromosome 10q24 in human (26). Therefore, the Dac mouse is considered to be the mouse model for SHFM3 in humans.

The Dac phenotype results from two different alleles, Dac[1J] and Dac[2J] (27). Both alleles arise from a disruption of the *dactylin* gene, which is a novel member of the F-box WD-40 protein family. F-box WD-40 proteins recruit specific target protein(s) through their WD-40 protein-protein binding domains for ubiquitin mediated degradation. The dactylin protein appears to function in maintaining the apical ectodermal ridge (AER) of the developing limb bud (27–29).

In humans, *DACTYLIN* has been mapped to the SHFM3 critical region (30) and is 87% identical to mouse *dactylin* at the nucleotide level. *DACTYLIN* is considered to be the best candidate gene for SHFM3 (27,30,31). To date, however, mutations in *DACTYLIN* have not been reported in sporadic cases of SHFM or familial cases mapping to the SHFM3 locus.

In this study, single-strand conformation polymorphism (SSCP) and sequencing analysis of the entire *DACTYLIN* coding region and flanking intronic sequences failed to detect mutations in affected individuals from six families linked to the SHFM3 locus. However, Southern analysis, pulsed field gel electrophoresis (PFGE) analysis and dosage analysis demonstrated complex rearrangements associated with large duplications of 10q24 in all six families and in an additional SHFM family in whom linkage analysis was not possible. These rearrangements create an extra copy of a portion of *DACTYLIN*, an extra copy of the complete β-*TRCP*, *POLL* and *LBX1* genes, and an extra copy of a sequence located ∼400–550 kb centromeric to *DACTYLIN* and constitute the first evidence of genomic abnormalities within the SHFM3 critical region.

RESULTS

DACTYLIN analysis by SSCP and sequencing

No mutations were detected by either SSCP or sequencing in an affected individual from each of the six SHFM3-linked families. In patient LS, a g1134 G→A (p378T→T) change

was identified in *DACTYLIN* exon 9. However, this neutral alteration was also found in a control individual.

Southern analysis

Southern analysis, using a variety of cDNA, exon-specific and intron-specific *DACTYLIN* probes, (Fig. 1A) was performed on an affected member of each linked family to screen for alterations or rearrangements that would have been missed by the SSCP and sequencing approaches. Altered bands were identified in three patients (DF, TU and LS; Fig. 1B).

In patient DF, the cDNA probe containing *DACTYLIN* exons 1–4 detected an altered band with eight different restriction enzymes (*Eco*RI, *Pst*I, *Bam*HI, *Bgl*I, *Bgl*II, *Hind*III, *Xba*I and *Bcl*I). Using different probes containing exon 4 on an E*co*RI filter, an extra 9 kb band was present in DF (Fig. 1B) and all affected members of the family, but was absent in the unaffected members and in 46 control individuals (Fig. 1C and data not shown). The *Eco*RI restriction map of the *DACTYLIN* gene identified a 6.4 kb fragment containing exons 2, 3 and 4 (Fig. 1A). This fragment alone was detected with a probe containing *DACTYLIN* exon 2, while the additional 9 kb band was detected with probes containing either exon 3 or exon 4 (Fig. 1A and B). Together, these results suggested that affected members of this family had a 10q24 genomic alteration in the 2.6 kb region between *DACTYLIN* exons 2 and 3 (Fig. 1A).

In patient TU, the *DACTYLIN* intron 5 probe detected an altered band with two different enzymes (*Eco*RI and *Pst*I). On a *Pst*I filter, this probe identified an extra 4.2 kb band (Fig. 1B) that segregated with the SHFM phenotype (data not shown). The *Pst*I restriction map of *DACTYLIN* identified a 5.4 kb fragment containing exon 5 and the region corresponding to the intron 5 probe (Fig. 1A). Only the normal band was detected with an exon 5 probe, thus localizing a genomic alteration in this family to the 2 kb region between the exon 5 and intron 5 probes (Fig. 1A).

In patient LS, the probe containing *DACTYLIN* exon 1 detected an altered band with three different enzymes (*Hpa*I, *Eco*RI and *Bcl*I). On an *Hpa*I filter, this probe identifed an extra 10 kb band (Fig. 1B) that was not detected in 46 control individuals (data not shown). The *Hpa*I restriction map of *DACTYLIN* identified a 14.9 kb fragment containing exon 1 (Fig. 1A). A probe located 10 kb upstream of exon 1, between the 5′ *Hpa*I site and exon 1, did not hybridize to the 10 kb band, thus localizing a genomic alteration to the 11 kb region between the *DAC* 5′ probe and exon 1 (Fig. 1A).

Southern analysis of patients DH, VB and AC did not reveal any altered bands using cDNA probes containing exons 1–4 or exons 4–8 on *Eco*RI, *Bam*HI, *Xba*I, *Hind*III, *Nco*I and *Nde*I filters.

Subgenomic library construction and characterization of a shifted band in patient DF

A subgenomic library for patient DF was constructed by cloning *Eco*RI genomic fragments, ranging from 8 to 10 kb, into a lambda vector in order to further characterize the 9 kb *Eco*RI fragment. Screening of this library with the *DACTYLIN* exon 4 probe identified a clone containing a 9.2 kb insert. Sequencing
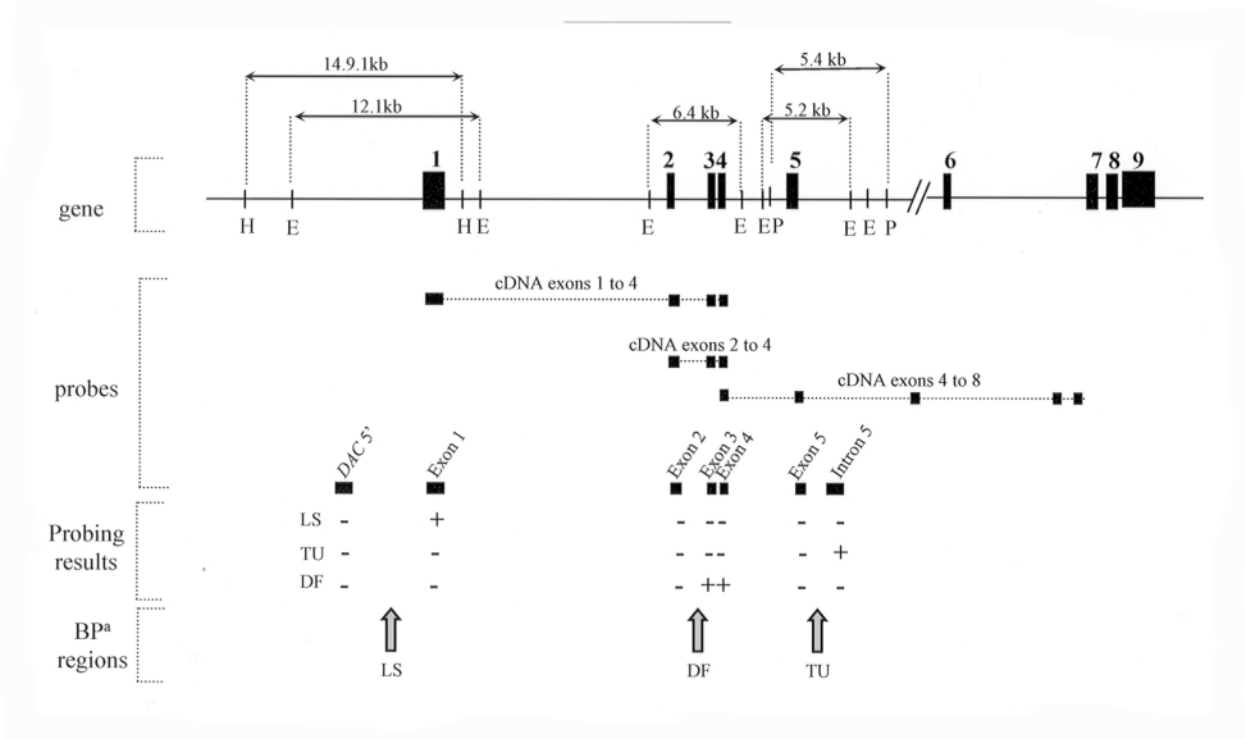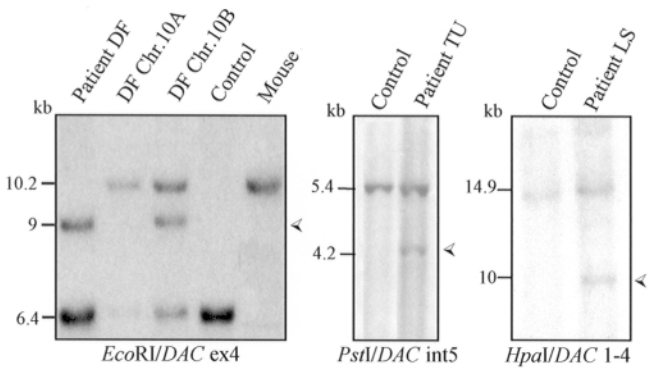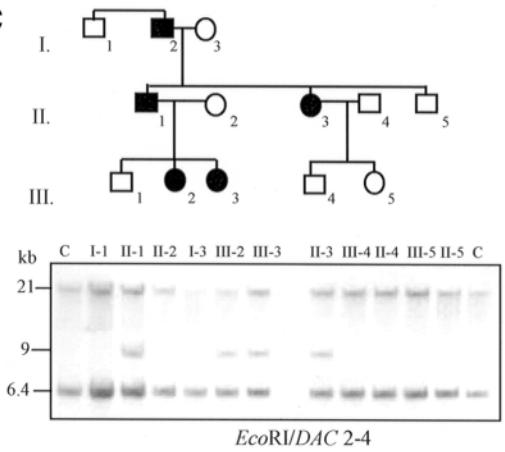
Figure 1. Southern analysis of SHFM patients DF, TU and LS. (**A**) Restriction map of the *DACTYLIN* gene (only the relevant enzyme sites are represented). E = *Eco*RI, P = *Pst*I and H = *Hpa*I. Scoring for presence (+) or absence (−) of the altered band using cDNA, exon-specific, and intron-specific *DACTYLIN* probes on an *Eco*RI filter localized the breakpoint (BP) region for each patient. (**B**) Southern hybridization of patients DF, TU and LS with probes *DAC* cDNA exon 4, *DAC* int 5 and *DAC* cDNA exons 1–4 respectively. The presence of an extra band in all three patients is indicated by the arrow. For patient DF, both the extra and control bands are present in the mouse–human monochromosomal hybrid cell line containing the affected chromosome (chromosome 10B), while only the normal band is present in the cell line containing the unaffected chromosome (chromosome 10A). The 10.2 kb band comes from mouse DNA. (**C**) Pedigree of DF's family and Southern hybridization with *DAC* exons 2–4 probe of an *Eco*RI filter. The 9 kb band is present only in the affected members of the family, which confirms segregation of the rearrangement within the family: solid symbols, affected individual; open symbols, normal.

of this clone revealed an extra 5.2 kb sequence adjacent to 4 kb of *DACTYLIN* sequence which contained exons 3 and 4, intron 3 and adjacent portions of introns 2 and 4 (Fig. 2A). The breakpoint in *DACTYLIN* was located at position 871 125 bp on contig NT_033229, 1620 bp 5′ of exon 3 (Fig. 2B). To confirm the rearrangement, PCR primers were designed in the new sequence and *DACTYLIN* intron 2 (Fig. 2A) and successfully amplified the expected 5.4 kb product in patient DF but not in a control individual (Fig. 2C). As additional confirmation, a probe to the extra 5.2 kb sequence (Cent1) hybridized to the 9 kb band previously detected with the *DAC* exon 4 probe in patient DF (Fig. 2D). Together, these data demonstrated the presence of an extra sequence disrupting the *DACTYLIN* gene between exons 2 and 3.

A BLASTN analysis (www.ncbi.nlm.nih.gov/blast) of this extra 5.2 kb sequence identified the BAC clone RP11-31L23
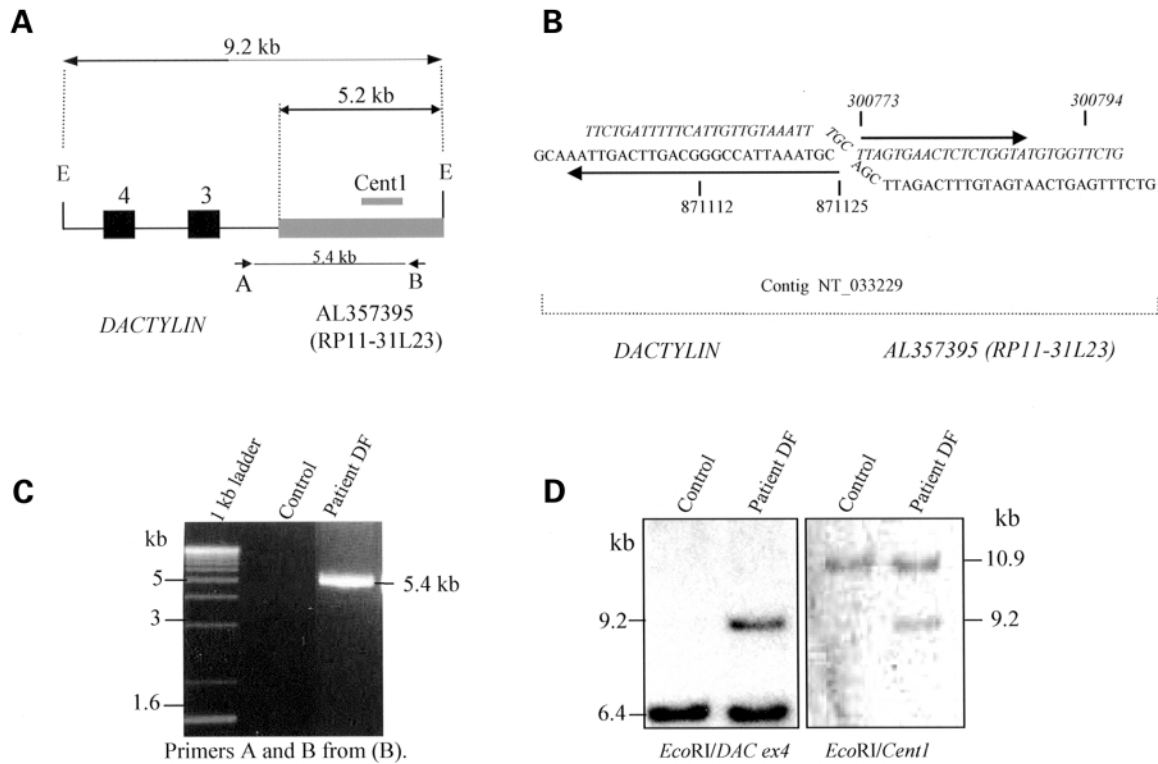
Figure 2. Characterization of the 9 kb altered band detected on an *Eco*RI filter in patient DF. (**A**) Schematic of the insert of the clone containing the 9.2 kb altered band (estimated to be 9 kb by Southern). An extra sequence of 5.2 kb, located ∼570 kb centromeric of the *DACTYLIN* gene, was adjacent to *DACTYLIN* intron 2. (**B**) Sequence of the breakpoint junction with the base pair position of the parental strand on the NT_033229 contig sequence. Sequence in italics represents the centromeric region located in database (AL357395). (**C**) PCR analysis using primer A (in the *DACTYLIN* gene) and B (in the centromeric sequence) from (A) revealed a PCR product of 5.4 kb only in patient DF but not in a control individual. (**D**) Southern blot analysis of *Eco*RI digested DNA from a control and patient DF using probe *DAC* exon 4 (left) or probe Cent1 located within the centromeric sequence (right). Both probes hybridize to the 9.2 kb band.

(GenBank no. AL357395), which is part of contig NT_033229 that also contains *DACTYLIN*. This extra sequence is ∼570 kb centromeric to *DACTYLIN*, and the centromeric breakpoint in patient DF was located at position 300 773 bp on contig NT_033229 (Figs. 2B and 3A) in what we now refer to as the centromeric region.

PFGE analysis

The rearrangements detected in patients DF, TU and LS were further characterized by PFGE analysis. In addition, the other SHFM patients were included in this analysis to complete the mutational screening of *DACTYLIN*.

On a *Nru*I filter, *DACTYLIN* cDNA probe *DAC* 4–8 (exons 4–8) detected extra fragments in patients DF, TU and LS, as anticipated from the Southern analysis, as well as in patients VB, DH and AC (Fig. 4A). For patient RH, a *DACTYLIN* exon 6 probe detected an extra fragment on an *Nru*I filter which was also present in his affected mother but absent in his unaffected father (data not shown). The altered fragments present in all seven SHFM patients were similar in size ranging from ∼550 to 610 kb (Fig. 4A) and none of these was detected in nine control individuals. In patients DF and TU, probe Cent1, located ∼550 kb centromeric to *DACTYLIN*, recognized the altered band previously detected with probe *DAC* 4–8 (Fig. 4A). In all seven SHFM patients, probe Cent2, located between

DACTYLIN and Cent1, hybridized to the extra fragments previously detected with *DACTYLIN* probes (Fig. 4A and B). Together these data suggested that the seven SHFM patients have a similar rearrangement involving the *DACTYLIN* gene and a sequence located ∼460 kb (Cent2)–570 kb (Cent1) centromeric to this gene.

Multiple hybridizations with probes located throughout the centromeric region and *DACTYLIN* were used to refine the breakpoint regions in each patient. Scoring of the presence or absence of the altered band narrowed the breakpoint locations in the centromeric and the *DACTYLIN* regions. A polymorphic band (c) of ∼550 kb was found in two controls and in patient AC using *DACTYLIN* probes and probes located 5′ of *DACTYLIN* (Fig. 4A). In patient AC, the altered band could be distinguished from this polymorphic band because of a significant difference in size resulting in a doublet (c and d) (Fig. 4A). However, in patients LS and VB the presence of this polymorphic band interfered with the scoring for presence/absence of the altered band derived from the rearrangement and previously detected with the Cent2 probe.

Identification of the breakpoint junction in patient TU

Additional probing of an *Mlu*I filter identified the centromeric breakpoint in patient TU within a 24 kb region between the probe Cent13 (289 044–289 478 bp of contig NT_033229) and
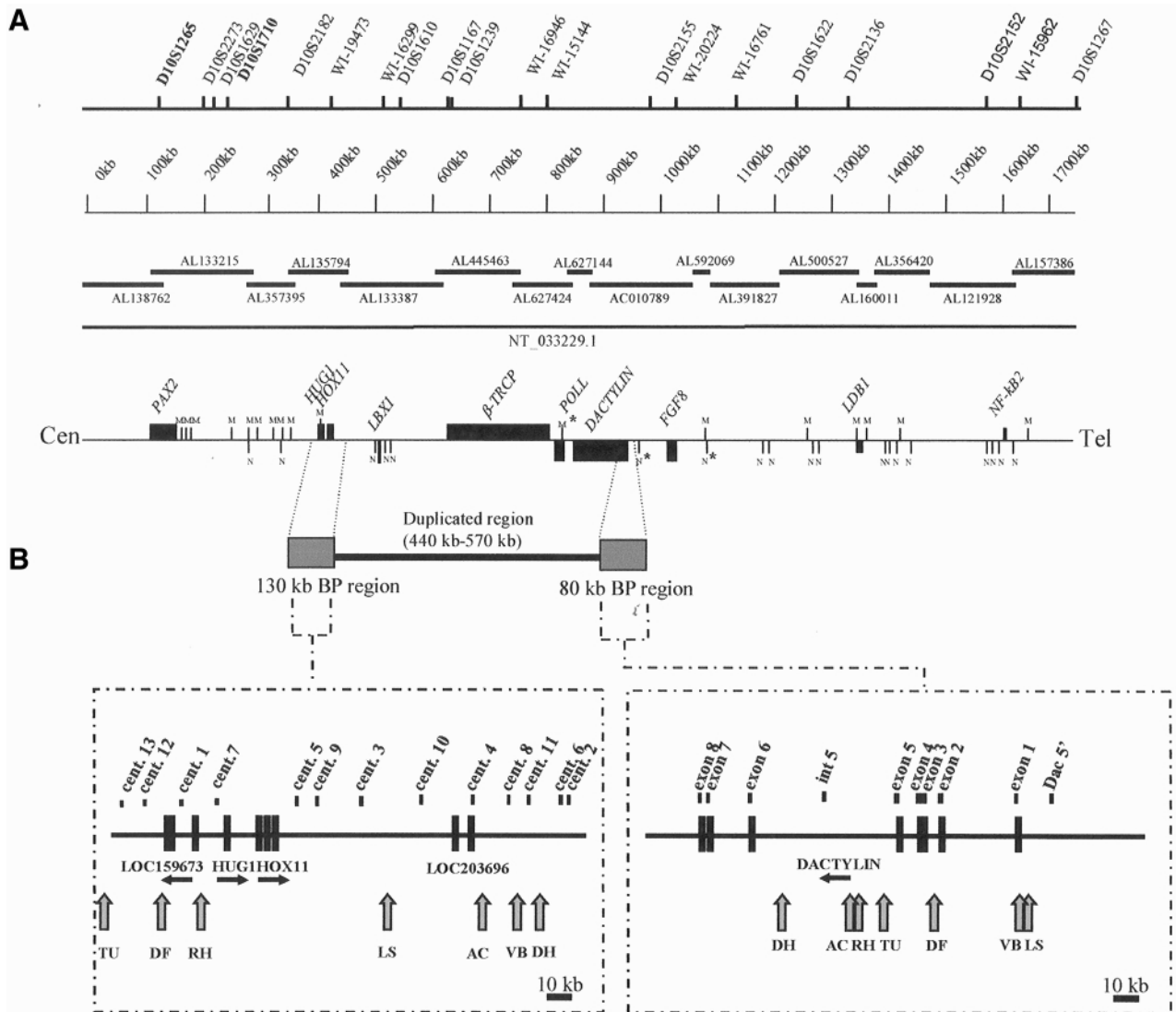
Figure 3. Computer-based sequencing of the *SHFM3* critical region and breakpoint locations. (**A**) From top to bottom: the position of the STS markers, the BAC clones with their accession number assembled into the NT_033229 contig. Only the SHFM3 possible candidate genes are represented. *PAX2*, *HUG1*, *HOX11*, β-*TRCP* and *NFkB2* are in a centromeric to telomeric orientation. *LBX1*, *DACTYLIN*, *FGF8*, *POLL* and *LDB1* are in telomeric to centromeric orientation. (**B**) location of the common duplicated region with the breakpoint (BP) regions (shaded boxed). The fine mapping of the breakpoint location for each patient is also represented (shaded arrows). Based upon the band sizes observed in the presence and absence of 5-azaC hypomethylating agent (data not shown), it was evident that the *Mlu*I site located between *DACTYLIN* and β-*TRCP* and the 2 *Nru*I sites 5′ of *DACTYLIN* are methylated (asterisk).

the next *Mlu*I site at position 264 876 bp (data not shown). Restriction map analysis of the 24 kb centromeric breakpoint region revealed 2 *Eco*RI and 2 *Pst*I sites that were in the middle of the region. Southern analysis in patient TU demonstrated the presence of an altered band on an *Eco*RI filter (2.5 kb) and a *Pst*I filter (4.2 kb) using the probe *DAC* int5 (Fig. 1B and data not shown). These findings suggested that the centromeric breakpoint is located in the vicinity of these *Eco*RI and *Pst*I sites. PCR analysis was then performed using a primer located within the centromeric region containing the *Eco*RI and *Pst*I sites and another primer located in intron 5 of *DACTYLIN*. A 2.1 kb band was amplified only from patient TU genomic DNA but not in DNA from two control individuals (data not shown). The sequence of this 2.1 kb band identified the breakpoint

junction between *DACTYLIN* and the centromeric sequence (data not shown). The *DACTYLIN* breakpoint was located at position 863 909 bp of contig NT_033229, 2 kb downstream of exon 5. The centromeric breakpoint was located at position 282 974 bp, 18 kb from the centromeric breakpoint in patient DF (Fig. 3B).

Based upon PFGE results in the other five patients, the *DACTYLIN* breakpoints are within a 78.7 kb region between the probe *DAC* 5′ (position 899 507–900 982 bp) and *DACTYLIN* exon 6 (position 820 652–820 913 bp; Fig. 3B). The centromeric breakpoints are within a 129.5 kb region between probe Cent6 (position 412 476–413 463 bp) and position 282 974 bp, the breakpoint identified in patient TU (Fig. 3B).
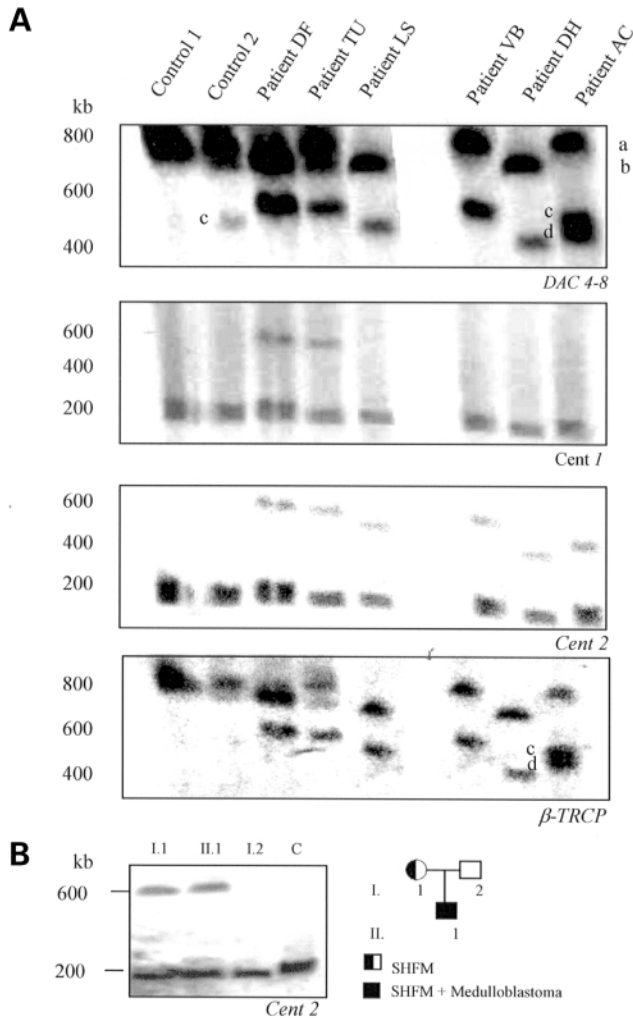
Figure 4. PFGE analysis of samples from seven SHFM patients, digested with *Nru*I. (**A**) Analysis of 6 SHFM patients (DF, TU, LS, VB, DH and AC) with probes *DAC* cDNA exons 4–8, Cent 1, Cent 2 and β-*TRCP* exon1 were used. The presence of two bands (a and b) around 800 kb is due to the presence of a methylated *Nru*I site located 5′ of the *FGF8* gene. A polymorphic band (c) is present in both control individual 2 and patient AC. Patient AC's altered band (d) is lower than the polymorphic band (c), resulting in the presence of a doublet (detected with *DAC* 4–8 and β-*TRCP* probes). For patients LS and VB, the distinction between the altered band (detected with Cent 2 or β-*TRCP* probes) and the polymorphic band could not be performed when using *DACTYLIN* specific probes. (**B**) Pedigree of RH's family and PFGE hybridization with Cent2 of a *Nru*I filter. The 600 kb band is only present in the affected mother and the proband, which confirms segregation of the rearrangement within the family.

Southern analysis of human–mouse hybrid cell lines

Dosage analysis of an *Eco*RI filter revealed that the intensity of the normal *DACTYLIN* band was two to three times greater than the intensities of either altered band detected in DF and TU (data not shown). This finding suggested that *DACTYLIN* was present in more than two copies in patients DF and TU. This possibility was further tested using hybrid cell lines generated from these two patients. For patient DF, all four hybrid cell lines carried only one chromosome 10: two carried the chromosome 10 arbitrarily called 'A' and two carried the chromosome 10 called 'B'. Chromosome 10B was considered

the affected chromosome since it contained DNA marker alleles segregating with the phenotype (data not shown). Southern analysis was performed with *Eco*RI and *Bam*HI using genomic DNA from a control individual and patient DF and DNA from two hybrids and a mouse fibroblast cell line (E2). On the *Eco*RI filter, a *DACTYLIN* exon 4 probe detected the extra 9 kb band and the normal 6.4 kb band in patient DF and cell line DF-Chr10B$_1$, while only the normal band was seen in the control individual and cell line DF-Chr10A$_1$ (Fig. 1B). An extra 10.2 kb band was seen only in the hybrid cell lines and in the mouse control because of cross hybridization with the *dactylin* mouse gene (Fig. 1B). On the *Bam*HI filter, the same probe detected the extra 15 kb band and the normal 30 kb band in patient DF and cell line DF-Chr10B$_1$, while only the normal band was seen in a control individual and cell line DF-Chr10A$_1$ (data not shown). The presence of both the normal and altered bands in DF-Chr10B$_1$ corresponding to the affected chromosome 10 suggested that at least a portion of *DACTYLIN* is duplicated on the affected chromosome in patient DF.

Interestingly, on both *Eco*RI and *Bam*HI filters, the Cent1 probe detected 2 bands (the normal band and an extra band) in patient DF and DF Chr10B$_1$, while only the normal band was detected in the control individual and DF-Chr10A$_1$ (data not shown). The presence of both bands in DF-Chr10B$_1$ suggested that the centromeric sequence is also duplicated on the affected chromosome in patient DF.

For patient TU, similar hybrids were created and Southern analysis was performed using *DACTYLIN* probes on *Pst*I and *Eco*RI filters. Both normal and shifted bands were detected in the hybrids containing the affected chromosome, while only the normal band was detected in the hybrids containing the unaffected chromosome (data not shown). As in patient DF, the results were consistent with the presence of a partial *DACTYLIN* duplication on the affected chromosome.

Dosage analysis by slot-blot

Although the hybrid cell line studies demonstrated the presence of an extra copy of a portion of *DACTYLIN* on the affected chromosome of patients DF and TU, the exact *DACTYLIN* copy number in these patients could not be determined by dosage analysis of the Southern blots. Dosage analysis using a slot-blot method (32–34) was undertaken to determine if a duplication of *DACTYLIN* existed independent of the rearrangement or if the extra copy of *DACTYLIN* resulted from the rearrangement.

Hybridization of a filter containing genomic DNA from DF and two control individuals with *DAC* exon 4 probe revealed a statistically significant increase of the slope in patient DF, suggestive of an extra copy of the *DACTYLIN* exon 4 region in this patient (Fig. 5B and data not shown). A 3:2 ratio was observed between the slope observed in patient DF and in a control individual. This indicated that three copies of this portion of *DACTYLIN* are present in patient DF and two copies are present in the control individual and a trisomy 21 control. A *DACTYLIN* intron 2 probe, located on the other side of the breakpoint, is not duplicated in patient DF since no significant differences between the slopes were detected (Fig. 5C and data not shown). Furthermore, probe Cent1 is also duplicated while probe Cent12, localized on the other side of the centromeric breakpoint, is not (Fig. 5D and E and data not shown). Further
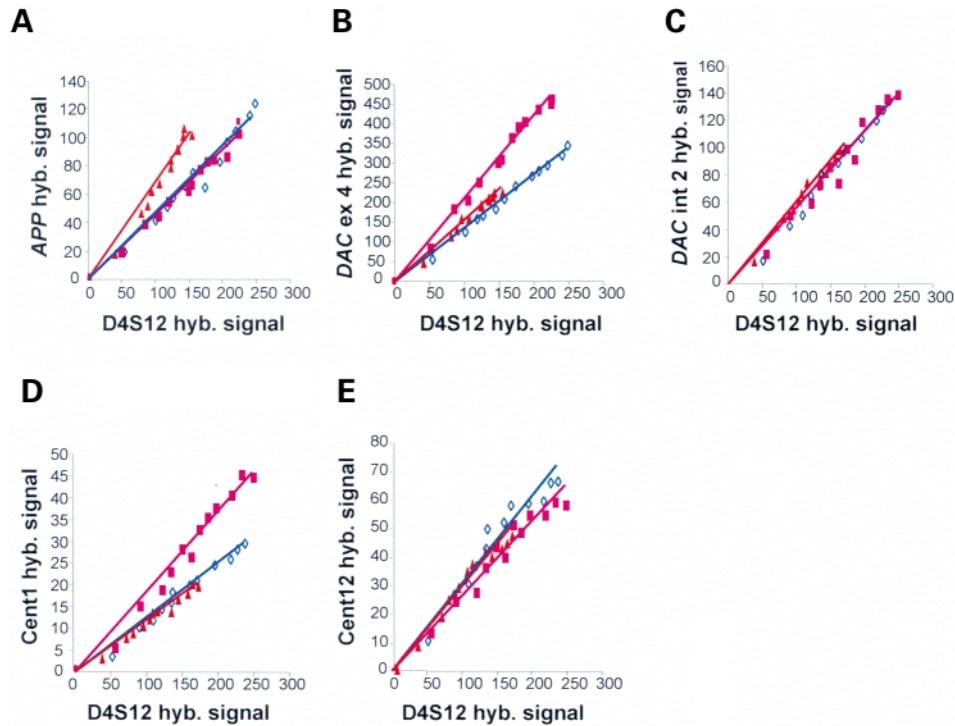
Figure 5. Graphical analysis of the densitometric values of test probes (*y* axis) vs the reference probe D4S12. In (**A**), the test probe is APP, a chromosome 21 specific probe; *DAC* exon 4 in (**B**); *DAC* intron 2 in (**C**), Cent1 in (**D**) and Cent12 in (**E**). (Diamond) Control; (Triangle) trisomy 21 individual; (Square) patient DF. In (A) the slope for the trisomy 21 patient is shifted, demonstrating duplication for the APP probe region in this patient. In (B) and (D) the slope for patient DF is shifted for probes *DAC* exon 4 and Cent1, respectively, but not for probes *DAC* intron 2 and Cent 12 in (C) and (E), respectively. The latter two probes are located on the other side of the *DACTYLIN* and centromeric breakpoints, respectively.

hybridization with a β-*TRCP* cDNA probe, located between *DACTYLIN* and Cent1, was performed and an increase of the slope was observed in patient DF (data not shown). Together, these data indicated that in patient DF the entire region between the *DACTYLIN* and the centromeric breakpoints is duplicated on the affected chromosome. This 570 kb duplicated region contains a portion of the *DACTYLIN* gene (exon 3 to the 3′-UTR), the complete β-*TRCP* and *POLL* genes as well as *LBX1*, *HUG1* and *HOX11* genes which are centromeric to *DACTYLIN*.

Slot blot analysis was then performed on the other six patients. In patients TU, LS, AC, DH and RH the region located between the *DACTYLIN* and centromeric breakpoints in each patient was also found to be present in three copies (data not shown). The dosage data were also used to narrow the *DACTYLIN* breakpoint region in patient VB that could not be determined by PFGE analysis.

DISCUSSION

A common genomic rearrangement was demonstrated to be associated with the SHFM phenotype in seven patients by using Southern, PFGE and dosage analyses as well as human–mouse hybrid cell lines containing a single chromosome 10 for two patients (DF and TU). The sequencing of the breakpoint junction in the same two patients revealed an extra sequence that is adjacent to *DACTYLIN*. This extra sequence is normally located ∼570 kb centromeric to *DACTYLIN*. In the other five

SHFM patients, the juxtaposition of both centromeric and *DACTYLIN* sequences was demonstrated by PFGE analysis. Additionally, Southern analysis of the single chromosome 10 hybrid cell lines of patients DF and TU and slot blot analysis of all seven patients demonstrated that the region located between the centromeric and *DACTYLIN* breakpoints is duplicated on one chromosome 10 in all the patients. Based on these findings, a model of an unequal recombination between the centromeric and *DACTYLIN* regions resulting in a tandem duplication is proposed to explain the rearrangement seen in these patients (Fig. 6). This model is consistent with the orientation of the sequences at the breakpoint junction, the size of the bands observed by PFGE and the duplication findings. The tandem duplication is likely the disease causing event for several reasons: (1) it segregates with the SHFM phenotype in the three families tested (DF, TU and RH); (2) the rearrangements detected in DF and LS were not detected in 46 control individuals; (3) the duplication is located on the affected chromosome, as demonstrated by the use of single chromosome 10 hybrid cell lines in patients DF and TU; and (4) none of the rearrangements detected by PFGE analysis in the seven SHFM patients was found in nine control individuals. Patient DH has the smallest duplicated region (440 kb) which defines the minimal duplicated region common to all patients. This narrows the number of genes included in the duplicated region to *LBX1*, β-*TRCP*, *POLL* and a portion of the *DACTYLIN* gene (exon 9 to exon 6) involving a region of ∼0.5 Mb (Fig. 6).
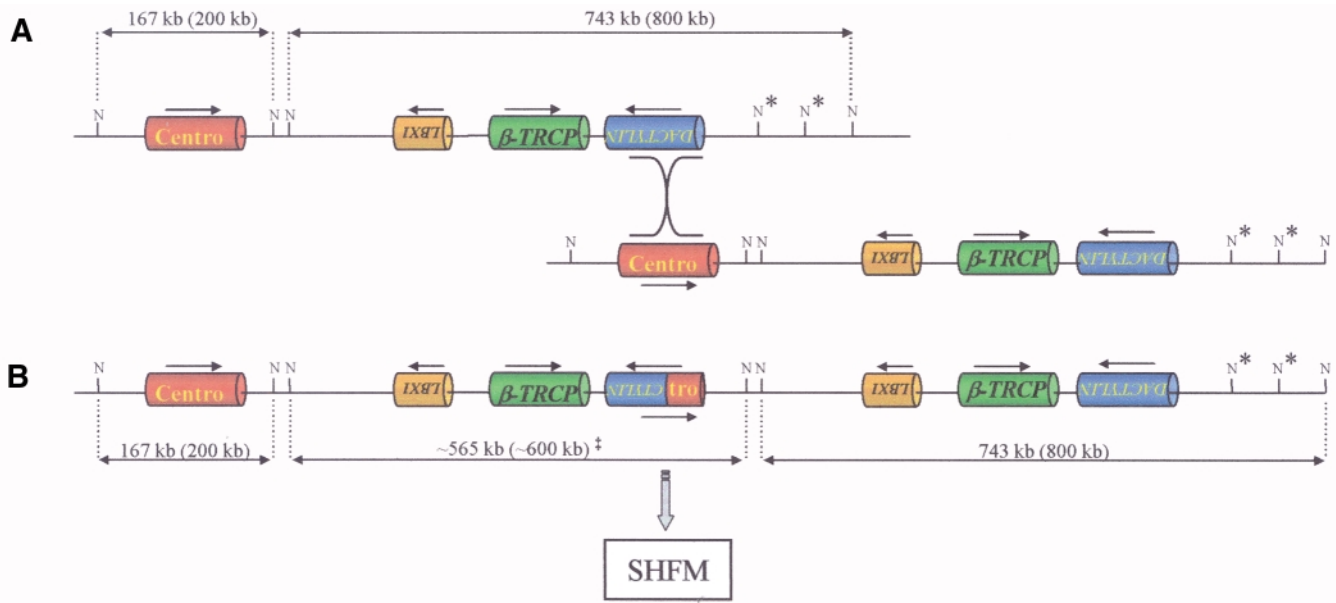
Figure 6. Model of the tandem duplication detected in the seven SHFM patients created by an unequal recombination between sequences of the centromeric region and sequences of the *DACTYLIN* gene region. (**A**) Misalignment of the *DACTYLIN* and the centromeric sequences. (**B**) Result of an unequal recombination between the *DACTYLIN* and the centromeric sequences. The expected sizes of the *Nru*I bands are indicated and the observed *Nru*I band sizes are indicated in brackets. The asterisks define the methylated sites. The double-dagger symbol defines the expected and observed extra *Nru*I fragment that is detected only in the SHFM patients.

Several other disorders have been reported to be associated with a submicroscopic duplication, deletion or inversion (35–37). These disorders are categorized as being genomic disorders in contrast to classic mendelian diseases (35). Regions of high similarity (>90% at the nucleotide level), known as low-copy repeats (LCRs), flank the genomic regions involved in the rearrangements (36,37). Indeed, misalignment and reciprocal recombination of these LCRs give rise to duplication, deletion or inversion of the regions flanked by these repeats (36–38). LCRs vary in size from 1 to 400 kb and can contain genes, pseudogenes, gene clusters or retroviral sequences. The tandem duplication detected in the SHFM patients suggests a similar mechanism for the rearrangements created by unequal crossing over events between highly similar regions of >1 kb and >90% identity. To look for LCRs in this region of chromosome 10, the 1.2 Mb of genomic sequence encompassing ~300 kb on either side of both breakpoint regions was analyzed using the DNA sequence comparisons program Miropeats (39). However, no evidence for the existence of such LCR sequences was identified, making it unlikely that LCRs mediate the rearrangements detected in the SHFM patients.

Several genomic rearrangements involving tandem duplications have been attributed to homologous recombination between *Alu* elements (40–45). *Alu* elements are the most abundant class of interspersed repeat sequences and represent 5–10% of the human genome. However, some regions that are prone to chromosomal rearrangement, like the chromosome 22q11 region, have more than 20% *Alu* elements. Using repeatmasker software (http://ftp.genome.washington.edu/cgi-bin/RepeatMasker), the repeat content of 100 kb of genomic sequence containing each breakpoint region was analyzed for interspersed repeat elements, and a high density of *Alu*

elements (~20%) was observed in both regions. This finding suggests that the rearrangement detected in the SHFM patients may be mediated by an unequal homologous recombination between *Alu* elements located in the centromeric and *DACTYLIN* regions. However, analysis of the sequence of the breakpoint junction in patients DF and TU did not detect any residual *Alu* elements common to both parental strands or within 50 bp of the junctions. This would suggest instead a non-homologous recombination that may still be mediated by the repetitive elements. The mechanism of non-homologous recombination is poorly understood. It is believed to be a two-step process with chromatid cleavage in the first step and rejoining in the second (46). This process would explain why no recombination hot-spots (<2 kb) were found in the seven SHFM patients in contrast with other disorders involving homologous recombination (47,48). However, the breakpoints were still relatively clustered within over a region of ~100 kb. It is likely that the high density of repetitive elements in the region is responsible for bringing together the centromeric and *DACTYLIN* regions that are >400 kb apart, consequently favoring non-homologous recombination.

How the duplication leads to the SHFM phenotype is unknown. *DACTYLIN* is the best candidate gene for SHFM3 because of its role in the *Dactylaplasia* mice phenotype (27), which is presumed to be the animal model for SHFM3 (26). The Dac phenotype results from one of two different alleles, Dac[1J] and Dac[2J] and both heterozygous mice for Dac[1J] and Dac[2J] have an identical phenotype (27). The evidence suggests that the Dac[2J] allele causes the Dac phenotype by abolishing the normal *dactylin* transcript and/or creating a novel transcript. However, it is unclear if the Etn transposon insertion in the Dac[1J] allele is the disease-causing mutation, since homozygote Dac[1J] mice expressed normal levels of the *dactylin* transcript

and no aberrant transcript was detected (27). In conjunction with this observation, our findings further question the role of *dactylin* in the Dac phenotype and *DACTYLIN* in human SHFM3, since they demonstrate partial *DACTYLIN* duplications in all patients tested. In five patients, extra *DACTYLIN* material is disrupted between exons 2 and 6 and in two patients the breakpoint is located no more than 8 kb upstream of the first exon. If *DACTYLIN* itself causes SHFM, it is possible that the rearrangements alter limb development by creating an aberrant *DACTYLIN* transcript that acts through a dominant negative mechanism. However, such a transcript has yet to be detected in our patients (data not shown) or in Dac[1J] mice (27).

Alternatively, the presence of a tandem duplication in the SHFM patients suggests that overexpression of another candidate gene may be responsible for the SHFM3 phenotype and possibly the Dac phenotype if *dactylin* itself is an innocent bystander in the Dac[2J] mouse. *LBX1* and β-*TRCP* are two potential candidate genes located in the duplicated region. *LBX1* is a homeobox gene and plays an important function in developmental processes (49). However, this gene is mainly expressed in the central nervous system and its expression in the limb bud is restricted to the early myogenic cells, likely ruling out this gene as responsible for SHFM3 (49–51).

β-*TRCP* is an F-Box-WD40 protein, like *DACTYLIN*, that is involved in the *NFkB* signaling transduction pathway. Several reports demonstrated a direct role of the *NFkB* pathway in limb development (52–56). Interestingly, three genes of the *NFkB* pathway (*IKKa*, *NFkB2* and β-*TRCP*) are within the critical region of SHFM3 defined by linkage mapping studies. *IKKa* knockout mice display severe limb and skin abnormalities. The *NFkB* pathway affects limb development by stimulating the expression of *SHH* and repressing the expression of *BMP4* in the underlying mesenchyme (52). Therefore, *NFkB* activity is likely critical for the maintenance of the apical ectodermal ridge (AER) by controlling the expression of SHH and BMP4. The *Dactylaplasia* mouse phenotype, and probably the SHFM3 phenotype in human, is caused by a defect in the maintenance of the AER (29). Overexpression of β-*TRCP* may disrupt *NFkB* activity giving rise to the SHFM3 phenotype. If this is the case, patients with trisomy of the 10q24 region, containing the β-*TRCP* gene should display an SHFM-like phenotype. One patient with a *de novo* tandem duplication 10q24–q26 most likely including the β-*TRCP* gene had mental retardation and characteristic facial features of the duplication 10q syndrome and minor malformation of the hands and feet (57). This patient had proximally implanted thumbs and toes, camptodactyly, a wide space between the first and second toes and syndactyly of the second and third toes (57). However, characteristic features of SHFM such as absence of the central digits and wide clefts in the hands/feet were not reported. Therefore, this patient does not seem to have a typical SHFM phenotype that would argue for a causative role of a dosage effect of β-*TRCP* in the SHFM3 phenotype. However, the existence of a modifier locus for SHFM3 (25) may complicate the phenotypical analysis of this patient; indeed this patient may not display a SHFM phenotype because of his genotype at the modifier locus.

A *cis*-acting positional effect may be another mechanism that would cause the SHFM3 phenotype by disrupting the expression of the genes flanking the breakpoints of the duplication. Interestingly, the 400 kb proximal and distal flanking regions harbor numerous candidate genes with known or putative roles in limb development (Fig. 3A). *FGF8* maps to the critical region of SHFM3 as defined by linkage mapping and its role in initiation, growth and patterning of the limb is extensively documented (58–60). However, direct sequencing and Southern analysis in SHFM3 patients did not reveal any mutations, ruling out this gene as the major cause of SHFM3 (61,62, Gurrieri and Schwartz, unpublished data). Suppressor of Fused (*SUFU*) is also located within the critical region and acts as negative regulator of the SHH pathway. However, *SUFU* mutations were recently found in patients with medulloblastoma (63) and no mutations were found among SHFM3 patients (62,64). *HOX11* is mainly expressed in T-cells and disruption of this gene caused acute lymphoblastic leukemia in a patient with a chromosomal translocation t(10;14) (65). More importantly, the *HOX11* murine homolog, *tlx1*, is not expressed in the limb bud and *tlx1* knockout mice did not display any limb phenotype, arguing against a causative role of *HOX11* (particularly through a loss of function mechanism) in SHFM3 (66).

Given the organization of the SHFM3 critical region, which contains multiple genes involved in the *NFkB* pathway and in limb development, it is conceivable that more than one gene in the region may be involved in the same pathway leading to SHFM. Hence, the Dac phenotype may be caused by two different mechanisms. For example, the Dac[2J] allele may cause limb malformation through loss of *dactylin* function and/or production of an aberrant transcript, while the Dac[1J] allele may cause increased dosage of a neighboring gene that normally downregulates *dactylin* or is downregulated by *dactylin*. In the families that we have studied, SHFM3 could result from either mechanism.

An important consequence of this study is the possible use of PFGE analysis with either *DACTYLIN* or centromeric probes for SHFM3 diagnosis. The novel *Nru*I fragment observed by PFGE analysis with the probe Cent2 may be the best approach for SHFM3 diagnosis. Indeed, probe Cent2 detected an altered fragment in all the SHFM patients and the distinction between the normal and altered bands was fairly easy to ascertain. However, PFGE analysis requires the use of lymphoblastoid cell lines and these are not always available. An alternative approach would be to perform dosage analysis of the region using slot blot analysis or real time quantitative PCR. These approaches were recently initiated in three other families linked to chromosome 10q24. In two of these, slot blot analysis using probes β-*TRCP* and *DACTYLIN* exon 6 demonstrated evidence of a duplicated fragment. In the third family, PFGE analysis using *DACTYLIN* exon 6 detected an extra band in an affected individual. Although further molecular characterization needs to be performed on these families, these preliminary data suggest a similar rearrangement with the other seven SHFM3 families.

This study raises several questions for future studies on SHFM3: (1) what is the mechanism of this rearrangement; (2) how common is this rearrangement among SHFM patients; and most importantly, (3) how does this rearrangement cause the SHFM3 phenotype? In a more general sense, this study reinforces the importance of Southern and PFGE screening to detect genomic rearrangements that can be missed by PCR-based approaches. These techniques will be essential for the

Table 1. Clinical features of the seven SHFM patients

Patient	Limbs[a]		Phenotype of the affected family members	Reference
	Hands	Feet		
DF	C, S	N/A[b]	Cleft hands/feet, oligodactyly, syndactyly	32
AC	S	C, S, O	Cleft hands/feet, oligodactyly, syndactyly	32
LS	O, S	C, S, O	Cleft hands/feet, oligodactyly, syndactyly	33
VB	N	C, S	Cleft hands/feet, oligodactyly, syndactyly, shortening of toes, duplication of digit 2	34
DH	N/A[b]	N/A[b]	Cleft hands/feet, oligodactyly, syndactyly	33
TU	D, T	C, S, O	Triphalangeal thumb, duplication of the thumb, nail hypoplasia	35
RH[c]	C, S, O	C, S, O	Affected mother has cleft hands and feet	This paper

[a]C = cleft; S = syndactyly; O = oligodactyly; N = normal; D = duplication of a digit; T = triphalangeal thumb.
[b]N/A = not available.
[c]This patient also had medulloblastoma.

identification of the rapidly growing family of genomic disorders.

MATERIALS AND METHODS

SHFM patients

All patients were ascertained for study based upon the presence of SHFM in one or more limbs. Informed consent was obtained prior to participation, and these studies were approved by the Institutional Review Committee of Self Regional Healthcare (Greenwood, SC, USA). Clinical details, pedigrees and linkage analysis of families of six of the seven patients (DF, AC, TU, LS, DH and VB) were previously described (18,24,62,67) and are summarized in Table 1. In all families, the phenotype was consistent with non-syndromic SHFM type I (6). Patient TU and some of his family members have thumb defects (duplicated and/or triphalangeal) with or without split feet. Patient RH has SHFM associated with medulloblastoma.

Analysis of SSCP

The sequence data from the full-length *DACTYLIN* cDNA (GenBank accession no. AF0281859) and genomic sequences from BAC clones RP11-190J1, RP11-148E14 and RP11-573E23 (GenBank accession nos AC010789, AL627144 and AL627424) were compared using the program Seqman 5.00$^{©}$ (DNASTAR Inc.) and Blast 2 sequence software (www.ncbi.nlm.nih.gov/Blast/). Divergence between the two sequences was taken to be indicative of the presence of an intron. BLAST analysis also identified a *DACTYLIN* pseudo-gene on chromosome 22q11. From the genomic structure, primers were designed to amplify the coding region of *DACTYLIN* for SSCP and sequence analysis. Primer sequences of the nine exons of the human *DACTYLIN* gene were designed using the program Primerselect 5.00$^{©}$ (DNASTAR Inc.). Individual exons, along with flanking intronic sequences, were amplified using 50 ng of genomic DNA in a total volume of 10 μl, containing 50 μM of each dNTPs, 1 μCi α^{32}dCTP, 1 μM of each primer and 0.5 units of *Taq* DNA polymerase (Sigma, St Louis, MO, USA). The PCR conditions were as follows: one

cycle at 95°C for 4 min; 20 cycles at 95°C for 30 s, annealing at 65–55°C (decrement of 0.5°C/cycle) for 30 s and elongation at 72°C for 30 s, then 15 cycles at 95°C for 30 s, 55°C for 30 s, 72°C for 30 s; one cycle at 72°C for 5 min. Five microliters of the radiolabeled PCR product were denatured with 5 μl of stop solution (95% formamide, 10 mM NaOH, 0.25% bromophenol blue, 0.25% xylene cyanol) at 94°C for 2 min before cooling on ice. Three microliters of the reaction mixture were loaded on a 0.5 × MDE^{TM} Acrylamide gel (FMC, Rockland, ME, USA) prepared following the manufacturer's procedure. Electrophoresis was performed at a constant power of 8 W for 19 h at room temperature. The gel was attached onto 3MM Whatman filter paper, and dried before exposure to X-ray Biomax film, (Kodak, Rochester, NY, USA) using standard techniques.

Sequencing

PCR products were either directly purified or gel-purified using the QIAquick PCR purification and gel extraction kit (QIAGEN, Valencia, CA, USA), and sequenced using the Thermosequenase Cy^{TM}5.5 Dye Terminator kit (Amersham Pharmacia Biotech, Piscataway, NJ, USA) and the forward or reverse exon-specific primer. A final purification was performed on Autoseq columns (Amersham Pharmacia Biotech, Piscataway, NJ, USA). All the samples were run on the automated laser fluorescence (ALF) DNA sequencer (Pharmacia Biotech, Piscataway, NJ, USA).

Southern analysis

Five micrograms of each patient's genomic DNA were singly digested overnight at 37°C using *Eco*RI, *Pst*I, *Dra*I, *Hind*III, *Xba*I, *Bcl*I, *Bgl*I, *Bgl*II, *Hpa*I, *Bam*HI and *Pvu*II enzymes (New England Biolabs$^{®}$ Inc., Beverly, MA, USA). After digestion, samples were electrophoresed on a 0.8% Seakem$^{®}$ LE agarose gel (BMA, Rockland, ME, USA) and transferred to a Nytran membrane (Schleicher and Schuell, Keene, NH, USA) using an alkaline downward transfer procedure (68). The filters were pre-hybridized for 2–3 h at 65°C in hybridization solution (4 × SSPE, 2 × Denhardt's solution, 0.5% SDS, 6% polyethyleneglycol, 40 μg/ml denatured sonicated salmon

sperm DNA) before adding the denatured probe. After 12–18 h of hybridization, filters were washed at 65°C, using a final wash of $0.1 \times$ SSC, 0.1% SDS. The filters were exposed to X-ray Biomax film (Kodak, Rochester, NY, USA), using standard techniques.

Subgenomic library construction

One-hundred and fifty micrograms of patient DNA was digested and electrophoresed using the same conditions as for the Southern analysis. The region containing the band of interest was cut out from the gel and the DNA was electroeluted and purified using Centricon® columns (Millipore Corporation, Bedford, MA, USA). The amount of DNA was quantified by UV (260 nm) detection and 0.2 µg were used in the ligation reaction containing 1 µg of the lambda zap express® vector (Stratagene, La Jolla, CA, USA). After packaging, the library was amplified and $\sim 5 \times 10^5$ to 1×10^6 plaques were plated, blotted and probed following the manufacturer's protocol (Stratagene, La Jolla, CA, USA).

Lymphoblastoid, human-mouse hybrid cell lines and DNA extraction

Epstein–Barr virus-transformed lymphoblastoid cell lines were established from controls and patients following a standard procedure (69). Human-mouse hybrid cell lines from patients DF and TU were generated using Conversion technology (GMP genetics Inc., Waltham, MA, USA). Genomic DNA was isolated from peripheral blood or from the cell lines by high salt precipitation (70). Purified DNA was diluted to a concentration of 105 ng/µl.

PFGE analysis

High molecular weight DNA was isolated in agarose plugs as previously described (71) using lymphoblastoid cell lines. The plugs were rinsed twice in 50 ml of TE buffer and then equilibrated for 30 min in 300 µl of the appropriate endonuclease restriction buffer. Excess buffer was removed and the plugs were incubated at the appropriate temperature for 16 h with 50 U of endonuclease enzyme per reaction (71). Single digestion of the DNA plugs was performed using *Not*I, *Mlu*I, and *Nru*I enzymes. Digested fragments in the range 50–500 kb were separated by electrophoresis on a 1% Seakem® Gold agarose gel (BMA, Rockland, ME, USA) at 200 V for 20 h, at 9°C in $0.5 \times$ TBE running buffer, using a 25 s pulse time on a Gene Navigator® apparatus (Amersham Pharmacia Biotech, Piscataway, NJ, USA). The separation of fragments 400–900 kb was accomplished by electrophoresis at 170 V for 24 h, at 9°C in $0.5 \times$ TBE buffer, using a 100 s pulse time.

DNA hybridization probes

DACTYLIN cDNA probes, containing exons 1–4 (*DAC* 1–4), exons 2–4 (*DAC* 2–4) and exons 4–8 (*DAC* 4–8) were generated by RT–PCR amplification of RNA extracted from a lymphoblastoid cell line from a control individual. Hybridization of individual exons was performed using PCR products generated with SSCP primers. The genomic sequence

corresponding to the *DACTYLIN* gene region (contig NT_033229.1) was submitted to the repeatmasker software available at http://ftp.genome.washington.edu/cgi-bin/RepeatMasker. Intronic probes were then developed using primers residing in non-repetitive sequences of the NT_033229.1 contig. Each intronic probe was amplified using 10 ng of BAC DNA when available or 100 ng of total genomic DNA extracted from a control individual. For intronic probes larger than 3 kb, long-range PCR was performed using *Taq* polymerase with buffer 1 from the Expand Long Template PCR system (Roche, Indianapolis, IN, USA) following the manufacturer's procedures. Prior to hybridization, intronic probes were preassociated with sonicated human placental DNA (Sigma, St Louis, MO, USA) in 50 000-fold excess, at 65°C for 90 min. All the PCR products used as probes were gel-purified with the QIAquick gel extraction kit (QIAGEN, Valencia, CA, USA) and sequenced. PCR products were labeled using the Radprime™ labeling system (Gibco-Invitrogen, Carlsbad, CA, USA) in the presence of 50 µCi of α^{32}dCTP (NEN, Boston, MA, USA).

Quantification of chromosome 10 sequences by slot-blot analysis

The slot-blot technique was used, with modifications, for the quantification of chromosome 10 sequences (32,33). In summary, DNA was quantified by a fluorescence-based assay using the dye PicoGreen® (Molecular Probes, Eugene, OR, USA). The DNA concentration was then adjusted to 50 ng/µl by dilution in 10 mM Tris–HCl buffer, pH 7.5, 1 mM EDTA and in 0.2 M of NaOH. The samples were incubated at 37°C for 20 min and 12 serial dilutions (0.2–1.5 µg) in 0.15 M NaOH and $0.1 \times$ SSC were blotted onto GeneScreen Plus® (NEN®, Life Science Products, Boston, MA, USA) using a slot blot apparatus (Minifold II; Schleicher & Schuell, Keene, NH, USA). After the DNA solution went through, each slot was washed with $2 \times$ SSC and the whole membrane was then rinsed in $2 \times$ SSC for 5 min and baked at 80°C for 20 min. Blots were probed with a reference probe, D4S12, prior to the hybridization with the test probes from chromosomes 21 and 10. All the probes were sequenced and tested by Southern hybridization to confirm their specificity and lack of hybridization to repetitive sequences. Band intensities were quantified using the Phosphoimager FUJIX BAS 1000 (Fuji Medical Systems, Stamford, CT, USA). The chromosome 10 signal (*y* axis) was then plotted against the reference probe signal (*x* axis) and the slopes were statistically analyzed and their comparison was assessed by *t*-test for significance as previously described (32,33).

To test the efficacy of the slot-blot method, DNAs from a control individual, patient DF and a trisomic 21 individual were used. Successive probing with a reference probe, D4S12 and a chromosome 21 probe, corresponding to the APP gene, revealed an extra copy of the APP gene only in the trisomic 21 patient. This was characterized by a statistically significant ($P < 0.001$) increase of the slope representative of the correlation between signals from the reference probe and the chromosome 21 probe (Fig. 6A).

ACKNOWLEDGEMENTS

REFERENCES

1. Calzolari, E., Manservigi, D., Garani, G.P., Cocchi, G., Magnani, C. and Milan, M. (1990) Limb reduction defects in Emilia Romagna, Italy: epidemiological and genetic study in 173,109 consecutive births. *J. Med. Genet.*, **27**, 353–357.

2. Nelson, K. and Holmes, L.B. (1989) Malformations due to presumed spontaneous mutations in newborn infants. *New Engl. J. Med.*, **320**, 19–23.

3. Froster-Iskenius, U.G. and Baird, P.A. (1989) Limb reduction defects in over one million consecutive live births. *Teratology*, **39**, 127–135.

4. Bod, M., Czeizel, A. and Lenz, W. (1983) Incidence at birth of different types of limb reduction abnormalities in Hungary 1975–1977. *Hum. Genet.*, **65**, 27–33.

5. Riano, G., I, Fernandez, T.J., Garcia, L.E., Moro, B.C., Mosquera, T.C., Rodriguez, F.A., Suarez, M.E., Ariza, H.F. and Franganillo, F.A. (2000) [Limb reduction defects in Asturias (1986–1997): prevalence and clinical presentation]. *An. Esp. Pediatr.*, **52**, 362–368.

6. Zlotogora, J. (1994) On the inheritance of the split hand/split foot malformation. *Am. J. Med. Genet.*, **53**, 29–32.

7. Roelfsema, N.M. and Cobben, J.M. (1996) The EEC syndrome: a literature study. *Clin. Dysmorphol.*, **5**, 115–127.

8. Temtamy, S.A. and McKusick, V.A. (1978) The genetics of hand malformations. *Birth Defects Orig. Artic. Ser.*, **14**, i-619.

9. Spranger, M. and Schapera, J. (1988) Anomalous inheritance in a kindred with split hand, split foot malformation. *Eur. J. Pediatr.*, **147**, 202–205.

10. Jarvik, G.P., Patton, M.A., Homfray, T. and Evans, J.P. (1994) Non-Mendelian transmission in a human developmental disorder: split hand/split foot. *Am. J. Hum. Genet.*, **55**, 710–713.

11. Ahmad, M., Abbas, H., Haque, S. and Flatz, G. (1987) X-chromosomally inherited split-hand/split-foot anomaly in a Pakistani kindred. *Hum. Genet.*, **75**, 169–173.

12. Zlotogora, J. and Nubani, N. (1989) Is there an autosomal recessive form of the split hand and split foot malformation? *J. Med. Genet.*, **26**, 138–140.

13. Faiyaz ul, H.M., Uhlhaas, S., Knapp, M., Schuler, H., Friedl, W., Ahmad, M. and Propping, P. (1993) Mapping of the gene for X-chromosomal split-hand/split-foot anomaly to Xq26–q26.1. *Hum. Genet.*, **91**, 17–19.

14. Gul, D. and Oktenli, C. (2002) Evidence for autosomal recessive inheritance of split hand/split foot malformation: a report of nine cases. *Clin. Dysmorphol.*, **11**, 183–186.

15. Scherer, S.W., Poorkaj, P., Allen, T., Kim, J., Geshuri, D., Nunes, M., Soder, S., Stephens, K., Pagon, R.A. and Patton, M.A. (1994) Fine mapping of the autosomal dominant split hand/split foot locus on chromosome 7, band q21.3–q22.1. *Am. J. Hum. Genet.*, **55**, 12–20.

16. Scherer, S.W., Poorkaj, P., Massa, H., Soder, S., Allen, T., Nunes, M., Geshuri, D., Wong, E., Belloni, E. and Little, S. (1994) Physical mapping of the split hand/split foot locus on chromosome 7 and implication in syndromic ectrodactyly. *Hum. Mol. Genet.*, **3**, 1345–1354.

17. Nunes, M.E., Schutt, G., Kapur, R.P., Luthardt, F., Kukolich, M., Byers, P. and Evans, J.P. (1995) A second autosomal split hand/split foot locus maps to chromosome 10q24–q25. *Hum. Mol. Genet.*, **4**, 2165–2170.

18. Gurrieri, F., Prinos, P., Tackels, D., Kilpatrick, M.W., Allanson, J., Genuardi, M., Vuckov, A., Nanni, L., Sangiorgi, E., Garofalo, G. *et al.* (1996) A split hand-split foot (SHFM3) gene is located at 10q24→25. *Am. J. Med. Genet.*, **62**, 427–436.

19. Celli, J., Duijf, P., Hamel, B.C., Bamshad, M., Kramer, B., Smits, A.P., Newbury-Ecob, R., Hennekam, R.C., Van Buggenhout, G., van Haeringen, A. *et al.* (1999) Heterozygous germline mutations in the p53 homolog p63 are the cause of EEC syndrome. *Cell*, **99**, 143–153.

20. Boles, R.G., Pober, B.R., Gibson, L.H., Willis, C.R., McGrath, J., Roberts, D.J. and Yang-Feng, T.L. (1995) Deletion of chromosome 2q24–q31 causes characteristic digital anomalies: case report and review. *Am. J. Med. Genet.*, **55**, 155–160.

21. Goodman, F.R., Majewski, F., Collins, A.L. and Scambler, P.J. (2002) A 117-kb microdeletion removing HOXD9-HOXD13 and EVX2 causes synpolydactyly. *Am. J. Hum. Genet.*, **70**, 547–555.

22. van Bokhoven, H., Hamel, B.C., Bamshad, M., Sangiorgi, E., Gurrieri, F., Duijf, P.H., Vanmolkot, K.R., van Beusekom, E., van Beersum, S.E., Celli, J. *et al.* (2001) p63 Gene mutations in eec syndrome, limb-mammary syndrome, and isolated split hand–split foot malformation suggest a genotype–phenotype correlation. *Am. J. Hum. Genet.*, **69**, 481–492.

23. Ianakiev, P., Kilpatrick, M.W., Toudjarska, I., Basel, D., Beighton, P. and Tsipouras, P. (2000) Split-hand/split-foot malformation is caused by mutations in the p63 gene on 3q27. *Am. J. Hum. Genet.*, **67**, 59–66.

24. Raas-Rothschild, A., Manouvrier, S., Gonzales, M., Farriaux, J.P., Lyonnet, S. and Munnich, A. (1996) Refined mapping of a gene for split hand–split foot malformation (SHFM3) on chromosome 10q25. *J. Med. Genet.*, **33**, 996–1001.

25. Chai, C.K. (1981) Dactylaplasia in mice a two-locus model for development anomalies. *J. Hered.*, **72**, 234–237.

26. Johnson, K.R., Lane, P.W., Ward-Bailey, P. and Davisson, M.T. (1995) Mapping the mouse dactylaplasia mutation, Dac, and a gene that controls its expression, mdac. *Genomics*, **29**, 457–464.

27. Sidow, A., Bulotsky, M.S., Kerrebrock, A.W., Birren, B.W., Altshuler, D., Jaenisch, R., Johnson, K.R. and Lander, E.S. (1999) A novel member of the F-box/WD40 gene family, encoding dactylin, is disrupted in the mouse dactylaplasia mutant. *Nat. Genet.*, **23**, 104–107.

28. Seto, M.L., Nunes, M.E., MacArthur, C.A. and Cunningham, M.L. (1997) Pathogenesis of ectrodactyly in the Dactylaplasia mouse: aberrant cell death of the apical ectodermal ridge. *Teratology*, **56**, 262–270.

29. Crackower, M.A., Motoyama, J. and Tsui, L.C. (1998) Defect in the maintenance of the apical ectodermal ridge in the Dactylaplasia mouse. *Dev. Biol.*, **201**, 78–89.

30. Ianakiev, P., Kilpatrick, M.W., Dealy, C., Kosher, R., Korenberg, J.R., Chen, X.N. and Tsipouras, P. (1999) A novel human gene encoding an F-box/WD40 containing protein maps in the SHFM3 critical region on 10q24. *Biochem. Biophys. Res. Commun.*, **261**, 64–70.

31. Sifakis, S., Basel, D., Ianakiev, P., Kilpatrick, M. and Tsipouras, P. (2001) Distal limb malformations: underlying mechanisms and clinical associations. *Clin. Genet.*, **60**, 165–172.

32. Rahmani, Z., Blouin, J.L., Creau-Goldberg, N., Watkins, P.C., Mattei, J.F., Poissonnier, M., Prieur, M., Chettouh, Z., Nicole, A. and Aurias, A. (1989) Critical role of the D21S55 region on chromosome 21 in the pathogenesis of Down syndrome. *Proc. Natl Acad. Sci. USA*, **86**, 5958–5962.

33. Blouin, J.L., Rahmani, Z., Chettouh, Z., Prieur, M., Fermanian, J., Poissonnier, M., Leonard, C., Nicole, A., Mattei, J.F. and Sinet, P.M. (1990) Slot blot method for the quantification of DNA sequences and mapping of chromosome rearrangements: application to chromosome 21. *Am. J. Hum. Genet.*, **46**, 518–526.

34. Delabar, J.M., Chettouh, Z., Rahmani, Z., Theophile, D., Blouin, J.L., Bono, R., Kraus, J., Barton, J., Patterson, D. and Sinet, P.M. (1992) Gene-dosage mapping of 30 DNA markers on chromosome 21. *Genomics*, **13**, 887–889.

35. Lupski, J.R. (1998) Genomic disorders: structural features of the genome can lead to DNA rearrangements and human disease traits. *Trends Genet.*, **14**, 417–422.

36. Inoue, K. and Lupski, J.R. (2002) Molecular mechanisms for genomic disorders. *A. Rev. Genom. Hum. Genet.*, **3**, 199–242.

37. Stankiewicz, P. and Lupski, J.R. (2002) Genome architecture, rearrangements and genomic disorders. *Trends Genet.*, **18**, 74–82.

38. Ji, Y., Eichler, E.E., Schwartz, S. and Nicholls, R.D. (2000) Structure of chromosomal duplicons and their role in mediating human genomic disorders. *Genome Res.*, **10**, 597–610.

39. Parsons, J.D. (1995) Miropeats: graphical DNA sequence comparisons. *Comput. Appl. Biosci.*, **11**, 615–619.

40. Stoppa-Lyonnet, D., Carter, P.E., Meo, T. and Tosi, M. (1990) Clusters of intragenic Alu repeats predispose the human C1 inhibitor locus to deleterious rearrangements. *Proc. Natl Acad. Sci. USA*, **87**, 1551–1555.

41. Pousi, B., Hautala, T., Heikkinen, J., Pajunen, L., Kivirikko, K.I. and Myllyla, R. (1994) Alu-Alu recombination results in a duplication of seven exons in the lysyl hydroxylase gene in a patient with the type VI variant of Ehlers-Danlos syndrome. *Am. J. Hum. Genet.*, **55**, 899–906.

42. Rudiger, N.S., Gregersen, N. and Kielland-Brandt, M.C. (1995) One short well conserved region of Alu-sequences is involved in human gene rearrangements and has homology with prokaryotic chi. *Nucl. Acids Res.*, **23**, 256–260.

43. Whitman, S.P., Strout, M.P., Marcucci, G., Freud, A.G., Culley, L.L., Zeleznik, L., Mrozek, K., Theil, K.S., Kees, U.R., Bloomfield, C.D. and Caligiuri, M.A. (2001) The partial nontandem duplication of the MLL (ALL1) gene is a novel rearrangement that generates three distinct fusion transcripts in B-cell acute lymphoblastic leukemia. *Cancer Res.*, **61**, 59–63.

44. Kutsche, K., Ressler, B., Katzera, H.G., Orth, U., Gillessen-Kaesbach, G., Morlot, S., Schwinger, E. and Gal, A. (2002) Characterization of breakpoint sequences of five rearrangements in L1CAM and ABCD1 (ALD) genes. *Hum. Mutat.*, **19**, 526–535.

45. Kolomietz, E., Meyn, M.S., Pandita, A. and Squire, J.A. (2002) The role of Alu repeat clusters as mediators of recurrent chromosomal aberrations in tumors. *Genes Chromosomes Cancer*, **35**, 97–112.

46. Hu, X.Y., Ray, P.N. and Worton, R.G. (1991) Mechanisms of tandem duplication in the Duchenne muscular dystrophy gene include both homologous and nonhomologous intrachromosomal recombination. *EMBO J.*, **10**, 2471–2477.

47. Pentao, L., Wise, C.A., Chinault, A.C., Patel, P.I. and Lupski, J.R. (1992) Charcot–Marie–Tooth type 1A duplication appears to arise from recombination at repeat sequences flanking the 1.5 Mb monomer unit. *Nat. Genet.*, **2**, 292–300.

48. Strout, M.P., Marcucci, G., Bloomfield, C.D., and Caligiuri, M.A. (1998) The partial tandem duplication of ALL1 (MLL) is consistently generated by Alu-mediated homologous recombination in acute myeloid leukemia. *Proc. Natl Acad. Sci. USA*, **95**, 2390–2395.

49. Jagla, K., Dolle, P., Mattei, M.G., Jagla, T., Schuhbaur, B., Dretzen, G., Bellard, F. and Bellard, M. (1995) Mouse Lbx1 and human LBX1 define a novel mammalian homeobox gene family related to the Drosophila lady bird genes. *Mech. Dev.*, **53**, 345–356.

50. Brohmann, H., Jagla, K. and Birchmeier, C. (2000) The role of Lbx1 in migration of muscle precursor cells. *Development*, **127**, 437–445.

51. Gross, M.K., Moran-Rivard, L., Velasquez, T., Nakatsu, M.N., Jagla, K. and Goulding, M. (2000) Lbx1 is required for muscle precursor migration along a lateral pathway into the limb. *Development*, **127**, 413–424.

52. Bushdid, P.B., Brantley, D.M., Yull, F.E., Blaeuer, G.L., Hoffman, L.H., Niswander, L. and Kerr, L.D. (1998) Inhibition of NF-kappaB activity results in disruption of the apical ectodermal ridge and aberrant limb morphogenesis. *Nature*, **392**, 615–618.

53. Hu, Y., Baud, V., Delhase, M., Zhang, P., Deerinck, T., Ellisman, M., Johnson, R. and Karin, M. (1999) Abnormal morphogenesis but intact IKK activation in mice lacking the IKKalpha subunit of IkappaB kinase. *Science*, **284**, 316–320.

54. Takeda, K., Takeuchi, O., Tsujimura, T., Itami, S., Adachi, O., Kawai, T., Sanjo, H., Yoshikawa, K., Terada, N. and Akira, S. (1999) Limb and skin abnormalities in mice lacking IKKalpha. *Science*, **284**, 313–316.

55. Li, Q., Lu, Q., Hwang, J.Y., Buscher, D., Lee, K.F., Izpisua-Belmonte, J.C. and Verma, I.M. (1999) IKK1-deficient mice exhibit abnormal development of skin and skeleton. *Genes Dev.*, **13**, 1322–1328.

56. Fisher, C. (2000) IKKalpha$^{-/-}$ mice share phenotype with pupoid fetus (pf/pf) and repeated epilation (Er/Er) mutant mice. *Trends Genet.*, **16**, 482–484.

57. Tomkins, D.J., Gitelman, B.J. and Roberts, M.H. (1983) Confirmation of a *de novo* duplication, dup(10) (q24 leads to q26), by GOT1 gene dosage studies. *Hum. Genet.*, **63**, 369–373.

58. Crossley, P.H., Minowada, G., MacArthur, C.A. and Martin, G.R. (1996) Roles for FGF8 in the induction, initiation, and maintenance of chick limb development. *Cell*, **84**, 127–136.

59. Lewandoski, M., Sun, X. and Martin, G.R. (2000) Fgf8 signalling from the AER is essential for normal limb development. *Nat. Genet.*, **26**, 460–463.

60. Moon, A.M. and Capecchi, M.R. (2000) Fgf8 is required for outgrowth and patterning of the limbs. *Nat. Genet.*, **26**, 455–459.

61. Ozen, R.S., Baysal, B.E., Devlin, B., Farr, J.E., Gorry, M., Ehrlich, G.D. and Richard, C.W. (1999) Fine mapping of the split-hand/split-foot locus (SHFM3) at 10q24: evidence for anticipation and segregation distortion. *Am. J. Hum. Genet.*, **64**, 1646–1654.

62. Tackels, D. (1996) Mapping of the third locus for split hand–split foot malformation, SHFM3. Clemson University.

63. Taylor, M.D., Liu, L., Raffel, C., Hui, C.C., Mainprize, T.G., Zhang, X., Agatep, R., Chiappa, S., Gao, L., Lowrance, A. *et al.* (2002) Mutations in SUFU predispose to medulloblastoma. *Nat. Genet.*, **31**, 306–310.

64. Grimm, T., Teglund, S., Tackels, D., Sangiorgi, E., Gurrieri, F., Schwartz, C. and Toftgard, R. (2001) Genomic organization and embryonic expression of Suppressor of Fused, a candidate gene for the split-hand/split-foot malformation type 3. *FEBS Lett.*, **505**, 13–17.

65. Hatano, M., Roberts, C.W., Minden, M., Crist, W.M. and Korsmeyer, S.J. (1991) Deregulation of a homeobox gene, HOX11, by the t(10;14) in T cell leukemia. *Science*, **253**, 79–82.

66. Raju, K., Tang, S., Dube, I.D., Kamel-Reid, S., Bryce, D.M. and Breitman, M.L. (1993) Characterization and developmental expression of Tlx-1, the murine homolog of HOX11. *Mech. Dev.*, **44**, 51–64.

67. Le Marec, B., Odent, S. and Treguier, C. (1990) Triphalangeal thumb and split foot in the same family. *Genet. Couns.*, **1**, 251–258.

68. Chomczynski, P. (1992) One-hour downward alkaline capillary transfer for blotting of DNA and RNA. *Anal. Biochem.*, **201**, 134–139.

69. Bolton, B.J. and Spurr, N.K. (1996) *Culture of Immortalized Cells.* Wiley-Liss, New York.

70. Schwartz, C.E., Ulmer, J., Brown, A., Pancoast, I., Goodman, H.O. and Stevenson, R.E. (1990) Allan-Herndon syndrome. II. Linkage to DNA markers in Xq21. *Am. J. Hum. Genet.*, **47**, 454–458.

71. Herrmann, B.G., Barlow, D.P. and Lehrach, H. (1987) A large inverted duplication allows homologous recombination between chromosomes heterozygous for the proximal t complex inversion. *Cell*, **48**, 813–825.